Agro-food waste upcycling into mycelium insulation: Linking structure with mechanical and fire performance

Materials Today Sustainability 33 (2026) 101295

Contents lists available at ScienceDirect

Materials Today Sustainability

journal homepage: www.journals.elsevier.com/materials-today-sustainability

Agro-food waste upcycling into mycelium insulation: Linking structure with mechanical and fire performance

Maryam Nejati [a,1], Li Zha [b,c,1], Rhoda Afriyie Mensah [d], Oisik Das [d], Antonio J. Capezza [e], Amparo Jiménez-Quero [b,c,*]

[a] Department of Molecular Biosciences, The Wenner-Gren Institute, SciLifeLab, Stockholm University, 106 91, Sweden
[b] Division of Industrial Biotechnology, Department of Life Sciences, Chalmers University of Technology, Göteborg, 412 96, Sweden
[c] Wallenberg Wood Science Center, Department of Life Sciences, Chalmers University of Technology, Göteborg, 412 96, Sweden
[d] Fire Technology Research Subject, Department of Civil, Environmental and Natural Resources Engineering, Luleå University of Technology, Luleå, 971 87, Sweden
[e] Polymeric Materials Division, Department of Fiber and Polymer Technology, School of Engineering Sciences in Chemistry, Biotechnology and Health, KTH Royal Institute of Technology, Stockholm, 100 44, Sweden

ARTICLE INFO

Keywords:
Fungal biocomposite
Ganoderma lucidum
Agro-food waste
Thermal insulation
Mechanical properties
Sustainable construction

ABSTRACT

This study presents a multiscale investigation of mycelium-based biocomposites produced via solid-state cultivation of *Ganoderma lucidum* on agro-food sidestreams. Three lignocellulosic residues, wheat bran (in two particle sizes), rice straw, and spent coffee grounds, were selected based on global availability and chemical diversity. The biocomposites were characterized to investigate how substrate composition and mycelial growth influence microstructure and macroscopic performance.

Monosaccharide analysis and scanning electron microscopy (SEM) revealed that wheat bran supported enhanced mycelial growth. Fine wheat bran-based composites exhibited compressive strengths up to 449 kPa at 30 % strain and tensile moduli of 15–25 MPa, significantly higher than expanded polystyrene (EPS), a conventional insulator. All biocomposites showed intrinsic surface hydrophobicity (water contact angles of 106–120°). Thermal analyses, including thermogravimetric analysis (TGA) and hot-plate conductivity measurement, confirmed their suitability as porous insulation. Cone calorimetry demonstrated improved fire safety in wheat bran-based composites, with reduced peak heat release rates (112–115 kW/m^2).

Embodied energy and carbon footprint assessments indicated up to 89 % lower energy demand and 72 % lower CO_2 emissions compared with EPS. Through multiscale characterization and direct benchmarking, this study shows how substrate selection and fungal-substrate interactions can be utilized to tailor performance. The findings provide insights into converting low-value biomass into scalable, fire-safer, and environmentally responsible insulation materials.

1. Introduction

Lignocellulosic biomass waste from agriculture or food is an underutilized resource worldwide [1]. For example, the annual production of rice and wheat straw waste in the world is approximately 670 and 710 million tons, respectively [2], posing significant disposal challenges. Today, most agricultural waste is either burnt or landfilled, which causes environmental pollution and greenhouse gas emissions [2], despite the potential to harness these materials as a cost-effective and renewable source for the production of valuable compounds and materials. Reusing agricultural waste will not only provide sustainable and environmentally friendly alternatives to unfavorable waste disposal routes, but also support the transition toward a circular bioeconomy. Thermochemical conversion routes such as pyrolysis, liquefaction, and gasification have been widely explored for lignocellulosic waste valorization [3]. These processes enable rapid conversion into fuels and carbon-rich materials but often require high temperatures and catalyst input [4]. Although relatively slower and requiring further study to achieve better control, biological conversion through fungi generally operates under mild conditions with low energy and chemical input. In this context, wood-decaying fungi such as Basidiomycota are particularly promising for transforming lignocellulosic biomass into functional

* Corresponding author. Division of Industrial Biotechnology, Department of Life Sciences, Chalmers University of Technology, Göteborg, 412 96, Sweden.
E-mail address: amparo@chalmers.se (A. Jiménez-Quero).
[1] Equal contribution.

https://doi.org/10.1016/j.mtsust.2025.101295
Received 12 September 2025; Received in revised form 19 November 2025; Accepted 23 December 2025
Available online 24 December 2025

biocomposites. These fungi can break down recalcitrant biomass and metabolize it into a tightly-knit mycelial matrix that embeds the lignocellulosic particles. This process imparts new properties to the original materials, which can be tailored by adjusting growth conditions and substrate specificity [5]. The vast diversity of fungal species and substrates enables the production of a wide range of final products, from foam-like structures to materials with properties comparable to hardwood [6].

The potential for designing bio-based materials, together with the versatility offered by different fungal-substrate combinations, is particularly relevant to the construction sector, which generates one of the largest waste streams in Europe [7]. In countries such as Sweden and the USA, it is also the second-largest consumer of plastics [8,9]. A significant portion of fossil-based materials in construction is used for insulation, with expanded polystyrene (EPS) being one of the most common materials [10]. However, EPS is non-renewable, non-biodegradable, flammable, and energy intensive to produce, emphasizing the need for sustainable, eco-friendly alternatives. Unlike EPS, fungi-based biocomposites produced from agri-food waste are biodegradable and free from hazardous chemicals. Their production requires relatively low energy, as most fungal species grow under moderate temperature conditions. These attributes position mycelium-based biocomposites as promising candidates for achieving a sustainable and circular insulation production process [11]. Previous studies have shown that such materials can reach performance levels comparable to conventional insulation products [6]. In addition, they exhibit intrinsic fire-retardant behavior due to the ability of mycelium to form a protective char layer during combustion [12], which can be further enhanced by incorporating silica- or lignin-rich additives [13]. Recent research on mycelium-based composites for insulation applications has advanced through rational design strategies such as molded textures, 3D-printed scaffolds, and engineered porous architectures, using substrates including bamboo fibers, wood, and cottonseed husk [14–17]. Although agro-food residues have occasionally been employed, few studies have systematically characterized their biochemical composition or related it to substrate recalcitrance, mycelial growth, and the resulting structure-property relationships. This lack of understanding limits the rational selection and optimization of waste-derived substrates for high-performance biocomposites.

To address this gap, this study investigates the use of representative agricultural residues with high global availability and waste management relevance. Wheat bran, a milling byproduct accounting for ~16 % of wheat grains, yields an estimated 100 million tons annually in the EU [18]. Rice straw contributes 800–1000 million tons per year globally, with 91 % produced in Asia [19], while spent coffee grounds generate ~6 million tons annually and pose notable disposal challenges due to their recalcitrance [20]. *Ganoderma lucidum*, a well-studied white-rot fungus capable of efficiently degrading lignocellulosic biomass and forming structurally coherent mycelial networks [21,22], was selected for its ability to produce composites with tunable mechanical and thermal properties. In this work, we systematically assess how substrate type, particle size, and cultivation temperature influence composition, microstructure, mechanical performance, and reaction-to-fire behavior of the final composites. Benchmarking against EPS, this work aims to develop bio-based insulation materials that are not only low-impact and circular, but also functionally competitive with fossil-based alternatives.

2. Experimental section

2.1. Materials

All used chemicals were purchased from Merck (Sweden) if otherwise specified. Potato Dextrose Broth (PDB) was prepared by adding 24 g/L of dry PDB powder to Milli-Q water (Elga Purelab, Option-Q), and the Potato Dextrose Agar (PDA) was prepared by adding 15 g/L agar (Duchefa Biochemie, Netherlands) to the PDB solution. Rice straw (RS) was obtained from the Dacsa group (Spain) and wheat bran (WB) was received from Lantmännen (Sweden). Rice straw particles displayed a fibrous morphology, with a mean width of approx. 0.9 mm, and length reaching up to 2–3 cm. In the case of WB, two particle sizes were used. The naturally occurring or medium-sized WB particles (mean equivalent circular diameter: 1.64 mm; median: 1.43 mm), derived from wheat milling waste, were employed. Subsequently, the same substrate was milled to achieve a finer particle size (mean equivalent circular diameter: 409 μm; median: 386 μm). Spent coffee ground (SCG, mean equivalent circular diameter: 562 μm; median: 484 μm) was prepared by brewing coffee (Arvid Nordquist, classic-Melllan) with a Moka pot using tap water. All substrates and media were autoclaved before use (Autoclave VWR Vapor line, Germany) at 121 °C and 15 psi for 20 min.

2.2. Biocomposite production

PDA cultures of *Ganoderma lucidum* (M9725) were prepared from the purchased kit (Mycelia, Belgium). After 5 days of incubation at 30 °C, 1 × 1 cm pieces of the resulting mycelium were cut and transferred on new PDA plates incubated at 25, 30, or 37 °C, and the growth progress was followed day-to-day. Furthermore, PDB cultures were prepared by adding 1 × 1 cm pieces of mycelium. These cultures were incubated at 25 and 30 °C to produce mycelia for compositional analysis.

Biocomposite production was started by activating *G. lucidum* from the kit. A mixture of kit mycelia, water, and barley bran-starch mix (2:1:1 v/v) was incubated at 30 °C for 5 days to produce the fungi stock. In the next step, solid-state cultures of *G. lucidum* were prepared on RS, medium and fine-sized WB, and SCG. This was done by mixing the fungi stock, water, and each of the substrates (2:1:2 v/v), thend incubating the resulting mixture at either 30 or 25 °C. After 8 days of growth, the cultures were dried at 60 °C overnight to inactivate the fungi and produce the final biocomposites. The weights of the biocomposites before and after drying at 60 °C were used to calculate the water loss in the drying process. Additionally, 1 × 1 cm pieces of each dried biocomposite were freeze-dried to determine the moisture content of each biocomposite.

2.3. Monosaccharide composition analysis

The monosaccharide composition of the substrates, biocomposites, and mycelia from PDB culture was analyzed by sulfuric acid hydrolysis as described by Martinez-Abad et al. [23]. 1 mg of each sample was weighed in triplicates and 125 μL of 72 % sulfuric acid was added to the dry samples. After 1 h at room temperature, 1325 μL of Milli-Q water was added, and the samples were incubated at 100 °C for 3 h. Afterward, the samples were filtered and diluted at 1:10 with Milli-Q water and further analyzed by high-performance anion exchange chromatography - pulsed amperometric detection (HPAEC-PAD, Dionex ICS-6000 DC Thermo Scientific, UK) using the Dionex CarboPac PA20 column. The elution was done at a constant flow of 0.4 ml/min at 30 °C and following a gradient of 1.2 % 200 mM NaOH to begin. After 18 min, the ratio of NaOH solution was increased to 100 %, which was constant for 20 min, and for the last 5 min, the composition ratio returned to 1.2 % of 200 mM NaOH. Fucose, arabinose, galactose, glucose, xylose, mannose, and glucosamine were used as standards.

2.4. Water contact angle

The contact angle was measured using the sessile drop method with a OneAttension Theta Lite instrument (Biolin Scientific, Sweden) equipped with a CCD camera (CAM200, KSV Instruments, Helsinki, Finland). A 4-μL droplet of Milli-Q water was placed on the surface of the biocomposite, and the contact angle was calculated from 20 images captured at a rate of one frame per second. The first 3 s of data were excluded to account for drop stabilization. Each sample was tested in triplicate, and the average contact angle and standard deviation were

reported.

2.5. Compression test

The compression test was performed according to the standard ASTM D1621-16 [24]. The samples were kept in a condition room at 50 % relative humidity for 72 h before the test. An Instron 5566 (Instron, double column, Norwood, MA, USA) with a 500 N load cell was employed. The dimensions of the cylindrical biocomposite samples were noted, and then they were compressed at a rate of 10 % of sample height per min. The test ended before reaching the maximum 500 N force or 80 % of the compressive strain. Triplicates of each biocomposite were tested, and the stress and strain were recorded automatically.

2.6. Tensile test

The tensile test was performed on Instron 5566, with the same preparation conditions as the compression test, based on ASTM D638 standard method [25]. Five to seven strips of 0.5 cm width were cut from the biocomposites, and the samples were fixed in two clamps with a gauge length of 2 cm. The strain rate was set at 0.2 cm per min. The test concluded upon sample rupture, with stress and strain data recorded automatically.

2.7. Thermogravimetric analysis (TGA)

The thermal stability of the materials was assessed on a TGA/SDTA851 (Mettler Toledo, Switzerland). Approximately 15 mg of the sample was weighed in alumina cups and heated from 50 °C to 900 °C at a heating rate of 10 °C/min. A purge of nitrogen gas at 50 mL/min flow was used to create an inert atmosphere.

2.8. Thermal insulation and reaction-to-fire test

The thermal conductivity of the mycelium materials was done using a modified hot-plate method partially based on the study performed by Blomfeldt et al. [26] The sample was cut into approximately 5 mm thick pieces with smooth, flat surfaces on all sides. Each piece was placed on a polished copper sheet to prevent infrared radiation from penetrating the sample via the underlying hot plate. The copper sheet was maintained at a constant temperature, establishing a thermal gradient of 11.8 K mm^{-1}. To prevent incorrect convection heating, the sample was surrounded by low thermal conductivity HI-70 Styrofoam, leaving only a minimal gap between the sample and the Styrofoam barrier. A plate thermometer was used to accurately measure the temperature of the hot plate surface and the sample. After allowing 10 min for thermal stabilization, five measurements were taken at 2-min intervals. The average temperature difference (ΔT) between the sample surface and the hot plate was used to calculate thermal conductivity based on $k = -q \cdot d_y/\Delta T$, where d_y is the sample thickness and q is the heat flux from the hot plate [27]. Using a TCC 918 cone calorimeter from Netzsch Analyzing & Testing, the reaction-to-fire characteristics e.g., peak heat release rate (PHRR), time to ignition (TTI), and total heat release (THR) of the specimens were evaluated. The samples were subjected to a heat flux of 35 kW/m^2. The test was carried out in accordance with ISO 5660–1:2015 standard [28].

2.9. Scanning electron microscopy (SEM)

The SEM samples were prepared by cryo-fracturing the biocomposites in liquid nitrogen. The fractured cross-sections were mounted on carbon conductive tape affixed to SEM stubs, which were stored in a desiccator for 24 h before sputter-coating with platinum/palladium using Cressington sputter coater, 208 HR. SEM images were captured with a Hitachi TM-1000 tabletop microscope at 10 kV voltage and 6 mm working distance. Hyphal diameters were calculated using ImageJ software (v. 1.53t) by averaging at least 50 diameter measurements from SEM images taken at various magnifications.

3. Results and discussion

3.1. Mycelium-based composites production

Although the optimal temperature range for the growth of *Ganoderma lucidum* is reported to be 25–35 °C, different strains exhibit varying performance within this interval [29]. In this study, fungal growth was evaluated at 25, 30, and 37 °C through daily visual inspection (Fig. S1). At 37 °C, mycelial growth was minimal and ceased by day 5, while both 25 and 30 °C supported active growth, with the most robust growth observed at 30 °C. These findings are consistent with Jayasinghe et al. [30], who identified 25–30 °C as the optimal cultivation range for *G. lucidum*. Consequently, biocomposites were produced at both 25 and 30 °C to assess the effect of temperature on growth and material properties. Table 1 listed the mycelium biocomposite sample codes along with their corresponding lignocellulosic substrates and incubation temperatures. Mycelial cultures on substrates were terminated on day 8. Subsequent thermal inactivation at 60 °C resulted in weight reductions of 17–65 %, primarily due to water loss. The final moisture contents of the dried biocomposites ranged from 1.2 % to 3.8 % (Table S1), below the 10 % threshold reported by Mardijanti et al. [31] for fungal inactivation, confirming the effectiveness of the drying process. The outer surfaces of the biocomposites were extensively covered by *G. lucidum* on day 8 (Fig. 1), though the extent of hyphal interpenetration varied by substrate (Fig. S3–5). In SCG-based biocomposites (Fig. S4–5, C & G), surface mycelia were dense, but particle interconnection was limited. This reflects the recalcitrant nature of SCG due to its high lignin content and compact grain structure, which may have restricted airflow and hindered further fungal penetration. RS-based substrates exhibited moderate mycelial colonization, with partial coverage on the underside (Fig. S4–5, D & H). The fibrous and loosely packed structure of RS may have influenced hyphal attachment and growth uniformity. Additionally, its relatively high lignin content and inherent surface hydrophobicity [32] likely affected water retention and fungal adhesion, leading to less interconnected networks compared to WB-based substrates. In fact, WB substrates, both fine and medium-sized (Fig. 1, S4-S5, A, B, E, and F), supported dense and uniform mycelial growth. As a less recalcitrant substrate, WB facilitated fungal growth, further aided by residual starch from industrial milling. While mycelial growth was sufficient at both 25 °C and 30 °C, the incubation temperature had a slight influence. This effect was particularly notable for SCG-based composites, where the underside view (Fig S5, C & G) showed more extensive mycelial development at 30 °C. This suggests that higher temperature may help overcome the substrate's high recalcitrance and limited oxygen diffusion.

3.2. Compositional analysis

Compositional analysis of the agri-food biomasses and the resulting biocomposites provided insight into carbohydrate utilization during biocomposite formation (Fig. 2, detailed in Table S2). The chart

Table 1
Sample codes of mycelium biocomposites with their lignocellulosic substrates and incubation temperatures.

Biocomposites	Starting substrate	Incubation temperature (°C)
FW-G-25	Fine-sized wheat bran	25
FW-G-30	Fine-sized wheat bran	30
MW-G-25	Medium-sized wheat bran	25
MW-G-30	Medium-sized wheat bran	30
C-G-25	Spent coffee grounds	25
C-G-30	Spent coffee grounds	30
R-G-25	Rice straw	25
R-G-30	Rice straw	30

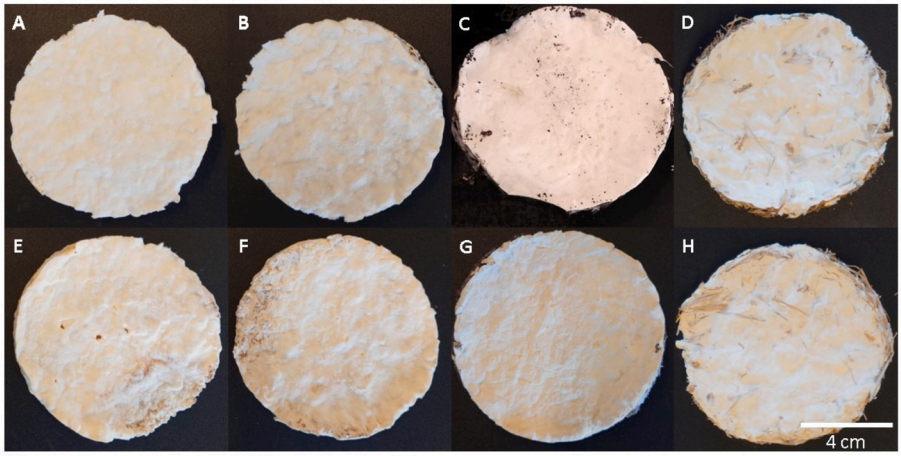

Fig. 1. Top-view of the biocomposites produced from solid-state cultures of *G. lucidum* on agro-food waste substrates at 25 °C (top row) and 30 °C (bottom row): (A, E) fine-sized wheat bran, (B, F) medium-sized wheat bran, (C, G) spent coffee grounds, and (D, H) rice straw.

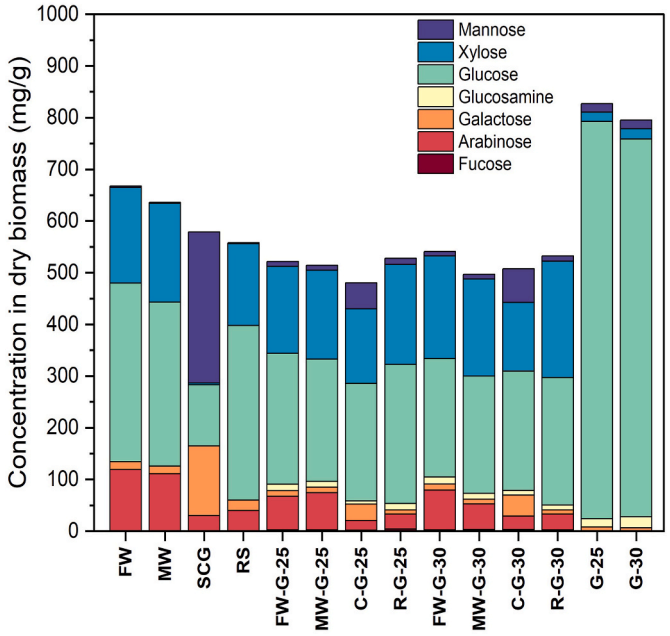

Fig. 2. Monosaccharide composition of the lignocellulosic substrates (FW, MW, SCG, RS) and their corresponding *G. lucidum* biocomposites grown at 25 °C and 30 °C, shown alongside neat mycelium controls (G-25, G-30).

illustrates the initial feedstocks (left), biocomposites prepared by solid-state cultivation (center), and neat mycelial biomass cultured in PDB by liquid-state cultivation (right). Glucose was the dominant monosaccharide in most samples, although its structural origin and distribution varied. A key marker distinguishing fungal biomass from plant-derived substrates was the presence of glucosamine, derived from fungal chitin, which served as an indicator of mycelial growth [33]. SCG-based biocomposites showed the lowest glucosamine contents (5.4 and 7.8 mg/g dry biomass in C-G-25 and C-G-30, respectively), indicating limited mycelial growth. This was likely due to limited oxygen diffusion within the densely packed SCG particles, as discussed previously. SCG is known to be rich in galactomannan (~50 %) and arabinogalactan (~15 %) [34], which corresponds to the elevated galactose and mannose levels in its carbohydrate profile. *G. lucidum* was able to utilize the soluble galactomannan fraction, resulting in the decline in galactose and mannose levels in C-G-25 and C-G-30 compared to raw SCG. However, fungal penetration was limited, likely due to the high lignin content (~40 %) that imparts structural recalcitrance [20]. In RS-based composites, glucosamine levels were higher: 10.9 mg/g in R-G-25 and 8.1 mg/g in R-G-30. These values suggest that *G. lucidum* can grow on more recalcitrant substrates under favorable conditions. Glucose in RS originates primarily from cellulose (~40 %) and hemicellulose (~25 %) rather than starch [32,35], and the combined presence of lignin and silica further limits accessibility to fungal degradation [36]. WB-based composites exhibited the highest glucosamine levels, reaching 11.7 mg/g in FW-G-30, indicating the most extensive mycelial growth, which was consistent with the observation that the mycelial network was more uniformly distributed in WB-based samples. According to Merali et al. [18], WB is composed mainly of arabinoxylan (~60 %), starch (~20 %), cellulose, and β-glucans, reflected in the arabinose, xylose, and glucose levels in Fig. 2. The presence of readily available starch supported rapid fungal growth, while the cellulose fraction contributed to the structural reinforcement of the resulting composites.

3.3. Surface hydrophobicity

Since biopolymer-based materials often suffer from hydrophilicity and moisture sensitivity, we next evaluated the surface hydrophobicity of the biocomposites to assess their suitability for insulation applications. The water contact angle results are summarized in Fig. 3, along with representative images captured. Contact angles above 90° are generally considered indicative of hydrophobic surfaces, while lower values suggest hydrophilicity [37]. All biocomposites exhibited hydrophobic behavior, with contact angles ranging from 106° to 120°, and no consistent trend related to substrate type or incubation temperature. For comparison, water contact angles are reported to be 92.9° for EPS foam [38] and 94° for flat polystyrene surfaces [39]. The inherent hydrophobicity is attributed to the surface coverage by fungal mycelia, particularly the presence of hydrophobins, the amphiphilic proteins secreted by *G. lucidum* that self-assemble at the air-water interface and lower the surface energy of fungal hyphae [40]. These proteins form rodlet layers or coatings that repel water, a mechanism that is conserved across many filamentous fungi. Since *G. lucidum* consistently covered the outer surfaces of all biocomposites, it is likely that this species-specific surface chemistry played a dominant role in determining wettability. Comparing with previous studies, Peng et al. [37] reported water contact angles of 76.3°–90.8° for *Pleurotus ostreatus*-based biocomposites, while Escaleira et al. [41] reported values of 116°–124° depending on the fungal strain. These comparisons support the idea that surface hydrophobicity is largely governed by fungal species, owing to differences in surface-active biomolecules, rather than substrate chemistry alone.

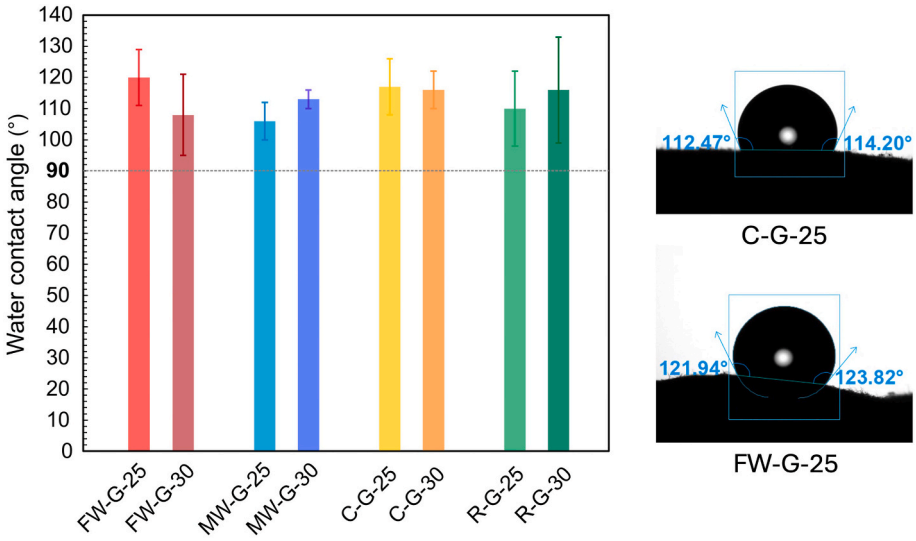

Fig. 3. Water contact angles of mycelium-based biocomposites grown on fine-sized wheat bran, medium-sized wheat bran, spent coffee grounds, and rice straw at 25 °C and 30 °C. Representative droplet images are shown for C-G-25 and FW-G-25.

3.4. Mechanical properties

Following the evaluation of surface properties, the mechanical behavior of the biocomposites was examined to assess their structural integrity and suitability for insulation applications. Representative stress-strain curves of the mycelium-based biocomposites in comparison with EPS during compression testing were shown in Fig. 4(a) and summarized in Table 2. No macroscopic fractures were observed during testing. Compressive strength did not vary significantly between biocomposites incubated at 25 °C or 30 °C ($p > 0.05$), suggesting limited influence of temperature under the tested conditions. While mycelial growth, indicated by glucosamine content, contributed to the mechanical integrity of the composites, it is not the sole determining factor. Samples with higher glucosamine levels, such as FW-G-25 (11.3 mg/g), FW-G-30 (11.7 mg/g), MW-G-30 (9.6 mg/g), and R-G-25(10.9 mg/g), generally exhibited higher Young's moduli (up to 43 kPa in FW-G-30), likely due to denser mycelial networks enhancing cohesion within the composite structure. However, exceptions such as MW-G-25, which showed high glucosamine (10.1 mg/g) but moderate stiffness (22 kPa), suggest that other factors, such as substrate distribution, packing, and density, also play a critical role in defining bulk compressive behavior. Indeed, substrate type had a stronger influence on compressive performance than particle size or incubation temperature. WB-based composites (FW-G-25, FW-G-30, MW-G-30) exhibited the highest stiffness (40–43 kPa), outperforming SCG-based samples (14–17 kPa), which indicated the importance of substrate-fungus interaction and composite morphology in achieving better mechanical performance of these biocomposites.

Table 2
Physical and mechanical properties from compression test of the biocomposites.

Composite	Density (kg/m^3)	Young's modulus (kPa)	Comp. stress at 10 % strain (kPa)	Comp. stress at 30 % strain (kPa)	Height recovery (2 h) (%)
FW-G-25	244 ± 10	40 ± 24	96 ± 46	449 ± 122	97 ± 8
MW-G-25	245 ± 11	22 ± 18	46 ± 25	194 ± 99	93 ± 5
C-G-25	330 ± 38	17 ± 2	38 ± 8	190 ± 27	80 ± 4
R-G-25	172 ± 5	37 ± 14	59 ± 27	160 ± 64	77 ± 2
FW-G-30	304 ± 17	43 ± 19	89 ± 49	430 ± 65	86 ± 3
MW-G-30	255 ± 7	41 ± 26	102 ± 41	346 ± 72	90 ± 7
C-G-30	323 ± 54	14 ± 4	44 ± 14	241 ± 55	98 ± 3
R-G-30	192 ± 46	27 ± 15	40 ± 17	170 ± 65	80 ± 6

Compressive strength at 30 % strain ranged from 160 to 449 kPa, comparable to similarly prepared mycelium composites, e.g., 270 kPa for *G. lucidum*-rapeseed cake and <150 kPa for *G. lucidum*-oat husk [42]. When benchmarked against EPS (Fig. 4(a)), all biocomposites demonstrated markedly higher stiffness and compressive strength within the same strain range. While EPS exhibited a gradual stress increase up to ~0.2 MPa at ~80 % strain, the mycelium-based biocomposites reached much higher stress values, up to ~0.8 MPa, at lower strains. This indicates that the biocomposites are considerably more resistant to compression, reflecting their more rigid and cohesive structure. Notably,

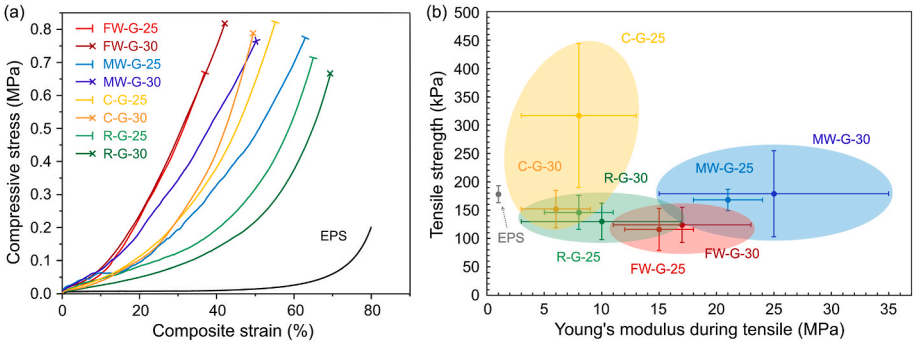

Fig. 4. (a) Representative compression stress-strain curves of mycelium-based biocomposites and EPS. (b) Tensile strength versus Young's modulus for the biocomposites, with EPS included for comparison.

composites based on fine-sized wheat bran showed the steepest curves, highlighting their superior load-bearing capacity among the tested formulations. The density of these composites (172–330 kg/m^3) places them within the medium-density foam category (100–400 kg/m^3) in the polymer foam context [43]. While higher density can contribute to improved compressive strength, this relationship is modulated by the structural heterogeneity of mycelium-based composites. Future improvements could focus on engineering the microstructure, for example, through directional porosity or hierarchical pore networks. One example of a hierarchical pore network was achieved by combining spores of *Trametes versicolor* with poplar sawdust [16]. Moreover, the integration of structurally complementary additives, such as cellulose nanofibrils, has proven effective for producing lightweight foams with enhanced structural properties [44].

The tensile mechanical properties of the biocomposites are summarized in Table 3 and visualized in Fig. 4(b), which plots tensile strength against Young's modulus for all formulations in comparison to EPS. All mycelium-based biocomposites exhibited higher tensile stiffness than EPS, with moduli ranging from 6 to 25 MPa, compared to ~1 MPa for EPS. However, their tensile strain at break remained limited (5–20 %), markedly lower than that of EPS (84 %). No consistent effect of incubation temperature was observed on tensile modulus or strength. Instead, both the substrate type and particle size played key roles in defining mechanical response. Medium-sized wheat bran (MW-G-30) yielded the highest tensile modulus (25 ± 10 MPa) and strength (179 ± 76 kPa), while fine-sized wheat bran composites (FW-G-25, FW-G-30) exhibited lower modulus and strength values (15–17 MPa, 116–124 kPa). This indicated the influence of substrate packing and structural cohesion during fungal growth. These findings are in agreement with Elsacker et al. [45], who emphasized the significant influence of substrate condition and particle size on tensile strength, rather than substrate chemical composition alone. SCG-based composites demonstrated unusually high tensile strength in some cases (e.g., C-G-25: 317 ± 127 kPa), though with low modulus and significant variability. As discussed previously, these composites suffer from weak fungal growth and potential particle detachment under tensile loading, leading to fracture dominated by the mycelial phase rather than cohesive biocomposite failure. Conversely, RS-based composites exhibited modest tensile moduli (8–10 MPa) and strengths (~130–146 kPa), consistent with limited mycelial growth and interfacial strength.

Compared to EPS, the biocomposites provided improved tensile stiffness and comparable or even higher strength, but with lower ductility. This reflects the contrasting failure mechanisms: EPS undergoes large deformation before failure, while the biocomposites fail in a more brittle manner due to their heterogeneous composition and limited plastic deformation. These findings highlight the importance of substrate morphology and fungal-substrate interfacial bonding in governing tensile behavior. Future work could target enhanced ductility and structural homogeneity, for instance by refining substrate particle gradation or introducing ductile biopolymeric additives to improve toughness without sacrificing stiffness.

Table 3
Mechanical properties from tensile test of the biocomposites in comparison with EPS.

Composite	Modulus (MPa)	Tensile stress at break (kPa)	Tensile strain at break (%)
FW-G-25	15 ± 3	116 ± 37	6 ± 2
MW-G-25	21 ± 3	168 ± 19	5 ± 1
C-G-25	8 ± 5	317 ± 127	20 ± 2
R-G-25	8 ± 3	146 ± 30	7 ± 3
FW-G-30	17 ± 6	124 ± 31	5 ± 1
MW-G-30	25 ± 10	179 ± 76	5 ± 2
C-G-30	6 ± 3	152 ± 33	15 ± 5
R-G-30	10 ± 7	130 ± 32	6 ± 3
EPS	1 ± 0	178 ± 15	84 ± 3

3.5. Thermal and insulation properties

Following the mechanical analysis, we next examine how the biocomposites respond to thermal exposure, as insulation materials must couple mechanical integrity with thermal stability and low heat transfer. We therefore evaluated their thermal degradation behavior and insulation performance to clarify how substrate composition and mycelial growth influence thermal stability and heat-transfer characteristics. Thermogravimetric analysis and first-derivative curves of the substrates and corresponding biocomposites are shown in Fig. 5, with onset and maximum degradation temperatures summarized in Table S3. The onset of weight loss was calculated automatically by the Mettler Toledo software based on the tangent-intersection method. The baseline corresponding to the initial region of constant mass was extrapolated, and a tangent was drawn along the steepest slope of the decomposition curve. The temperature at the intersection of these two lines was defined as the onset of thermal degradation. According to Sakhiya et al. [46], hemicellulose and cellulose typically decompose at 220–330 °C and 300–400 °C, respectively, while lignin degrades gradually over a broader temperature range (160–900 °C). Among the raw substrates, SCG and RS exhibited higher onset and peak degradation temperatures in DTG, consistent with their higher lignin content and overall recalcitrance. In contrast, WB-based substrates decomposed earlier, reflecting their lower thermal stability and greater digestibility. Upon mycelial growth, a downward shift in the main DTG peaks was observed across all composites. WB-based biocomposites exhibited the largest shifts (13–15 °C), suggesting enhanced degradation of carbohydrate fractions by *G. lucidum*. Smaller shifts (~5 °C) were observed in SCG- and RS-based composites, consistent with their higher resistance to fungal breakdown. These results reinforce the compositional data (Fig. 2), highlighting more extensive mycelial growth in WB-based mycelium composites. The onset temperatures for weight loss in biocomposites ranged from 250 to 269 °C, lower than those of their respective substrates. Although this indicates reduced thermal stability at elevated temperatures, all composites remained stable below 250 °C, meeting the thermal tolerance required for most insulation applications. In comparison, EPS undergoes rapid degradation starting at 340 °C, with peak decomposition around 450 °C [47]. While EPS exhibits higher thermal stability, its combustion can release toxic volatiles [12,48]. In contrast, mycelium-based biocomposites may offer safer degradation profiles due to their bio-based nature and char-forming tendency under fire exposure.

The thermal conductivity of the biocomposites was also evaluated to assess their suitability for insulation applications. As shown in Table 4, all composites exhibited values within a range of 0.099–0.124 W m^{-1} K^{-1}. No clear trend was observed in relation to substrate type or incubation temperature, as the measured values were comparable across all conditions. A recent comprehensive review on the thermal conductivities of mycelium-based composites reported values ranging from 0.026 to 0.18 W m^{-1} K^{-1}. Specifically, *Ganoderma lucidum*-based composites typically exhibit conductivities between 0.045 and 0.085 W m^{-1} K^{-1} [49]. Lower conductivity is generally achieved through reduced density, the use of substrates with intrinsically low thermal conductivity, and the formation of an intact fungal skin. In comparison, EPS demonstrates excellent insulation performance, with reported conductivities of approximately 0.036–0.046 W m^{-1} K^{-1} [50]. Interestingly, the thermal conductivity of a neat *Ganoderma* mycelium skin has been recently reported to be as low as 0.015 W m^{-1} K^{-1} [51]. These findings highlight two key aspects to achieve better insulation properties: density reduction of these biocomposites remains crucial, and understanding substrate-species interactions to achieve a controlled porous architecture with continuous mycelial coverage is beneficial.

3.6. Microstructure

Since varying the cultivation temperature (25 °C vs. 30 °C) did not

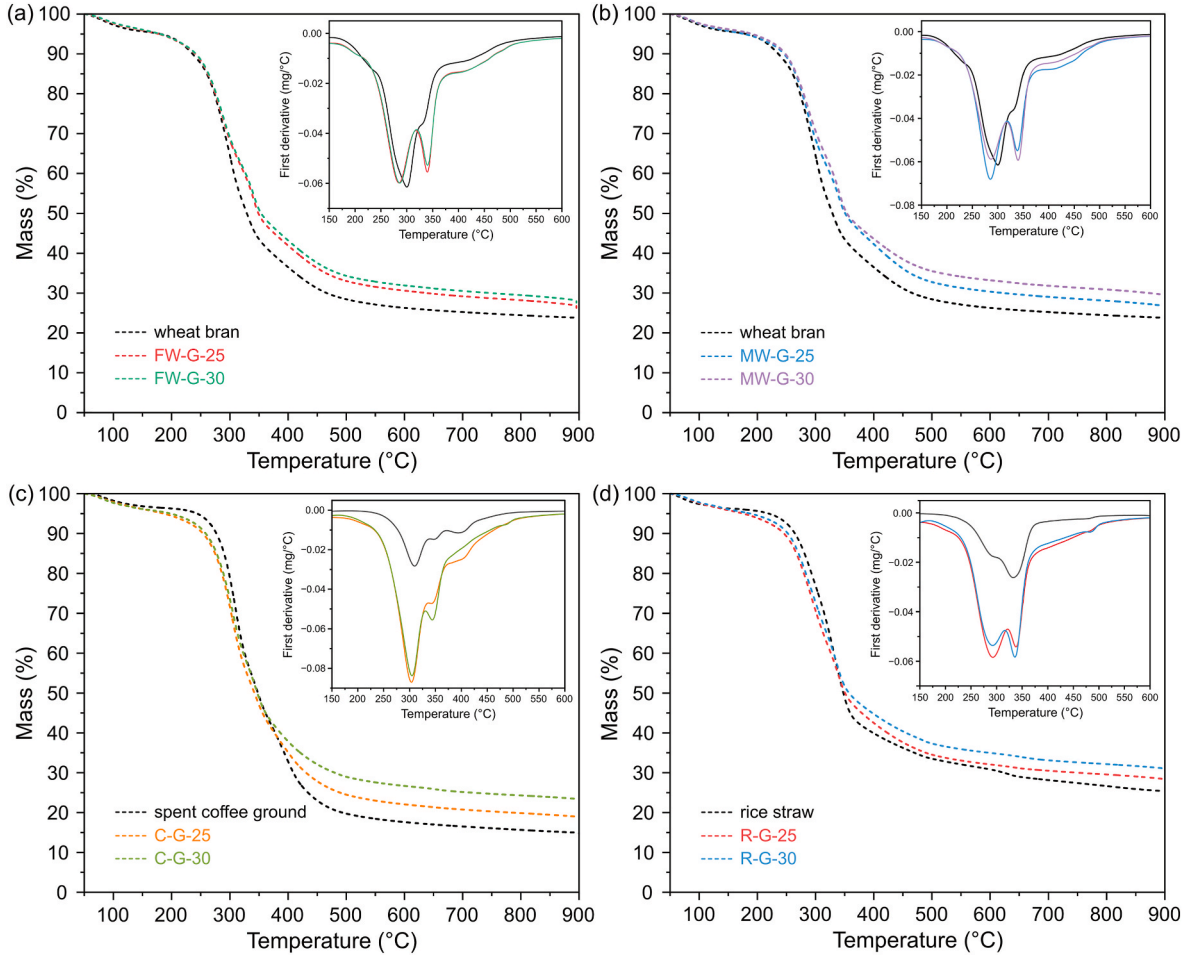

Fig. 5. Thermogravimetric analysis (dashed lines) and derivative thermogravimetry (solid lines) of the substrates and corresponding biocomposites produced at 25 °C and 30 °C. (a) Wheat bran and fine-sized wheat bran biocomposites, (b) wheat bran and medium-sized wheat bran biocomposites, (c) spent coffee grounds and corresponding biocomposites, and (d) rice straw and corresponding biocomposites.

Table 4
Thermal conductivities of the biocomposites.

Biocomposites	Thermal Conductivity ($W \cdot m^{-1} \cdot K^{-1}$)
FW-G-25	0.107 ± 0.003
FW-G-30	0.108 ± 0.002
MW-G-25	0.099 ± 0.001
MW-G-30	0.124 ± 0.001
R-G-25	0.109 ± 0.019
R-G-30	0.109 ± 0.002
C-G-25	0.105 ± 0.012
C-G-30	0.106 ± 0.007

markedly affect the hydrophobic, mechanical, or thermal performance of the composites, subsequent analyses of microstructure and fire performance were confined to the composites prepared at 25 °C. This temperature was selected as it closely reflects ambient conditions and provides a more energy-efficient processing route. The internal architecture of the biocomposites was then investigated by SEM to study the relationship between composition, microstructure, and macroscopic properties. Based on the SEM images (Fig. 6) and quantitative mycelial diameter measurements (Table S4), the microstructural features of the mycelium-based biocomposites varied substantially depending on substrate type, reflecting differences in mycelial growth and interfacial interaction. Among all samples, FW-G-25 and MW-G-25 exhibited denser and more cohesive mycelial network. The hyphae formed interconnected and layered structures with extensive branching, closely entangled with the wheat bran substrate. This is evident in the SEM images, where regions of seamless hypha-substrate interaction suggest strong interfacial bonding. Quantitatively, FW-G-25 showed the largest main hyphal diameter (1.54 ± 0.58 μm) and high branch density (branch diameter 0.23 ± 0.06 μm), consistent with the high glucosamine content and superior mechanical properties observed previously. In MW-G-25, while mycelial networks remained well-developed, the hyphae exhibited thinner diameters (0.98 ± 0.21 μm for main hyphae, 0.18 ± 0.03 μm for branches). These results suggest that substrate packing density and particle size can influence hyphal architecture and spatial distribution, which likely affects both mechanical stiffness and toughness. In contrast, C-G-25 and R-G-25 showed markedly looser microstructures with reduced mycelial connectivity and limited hypha-substrate interaction. In SCG-based composites, the hyphae appeared more fragmented and irregular, with a high degree of local bending and branching (main diameter 0.85 ± 0.20 μm; branch diameter 0.29 ± 0.13 μm), but poor cohesion with the particulate substrate. This supports the notion that SCG's compactness and lignin-rich composition hinder deep mycelial penetration. Similarly, the RS-based composites exhibited low hyphal density and extremely low degree of branching, with the lowest measured hyphal diameter (0.82 ± 0.17 μm), reflecting limited growth. Together, these microstructural observations support the macro-scale mechanical performance trends: wheat bran substrates enabled well-integrated hyphal matrixes that enhance load-bearing capacity, while spent coffee ground and rice straw substrates led to more fragmented and discontinuous architectures. These findings highlight the role of substrate digestibility and porosity in guiding mycelial

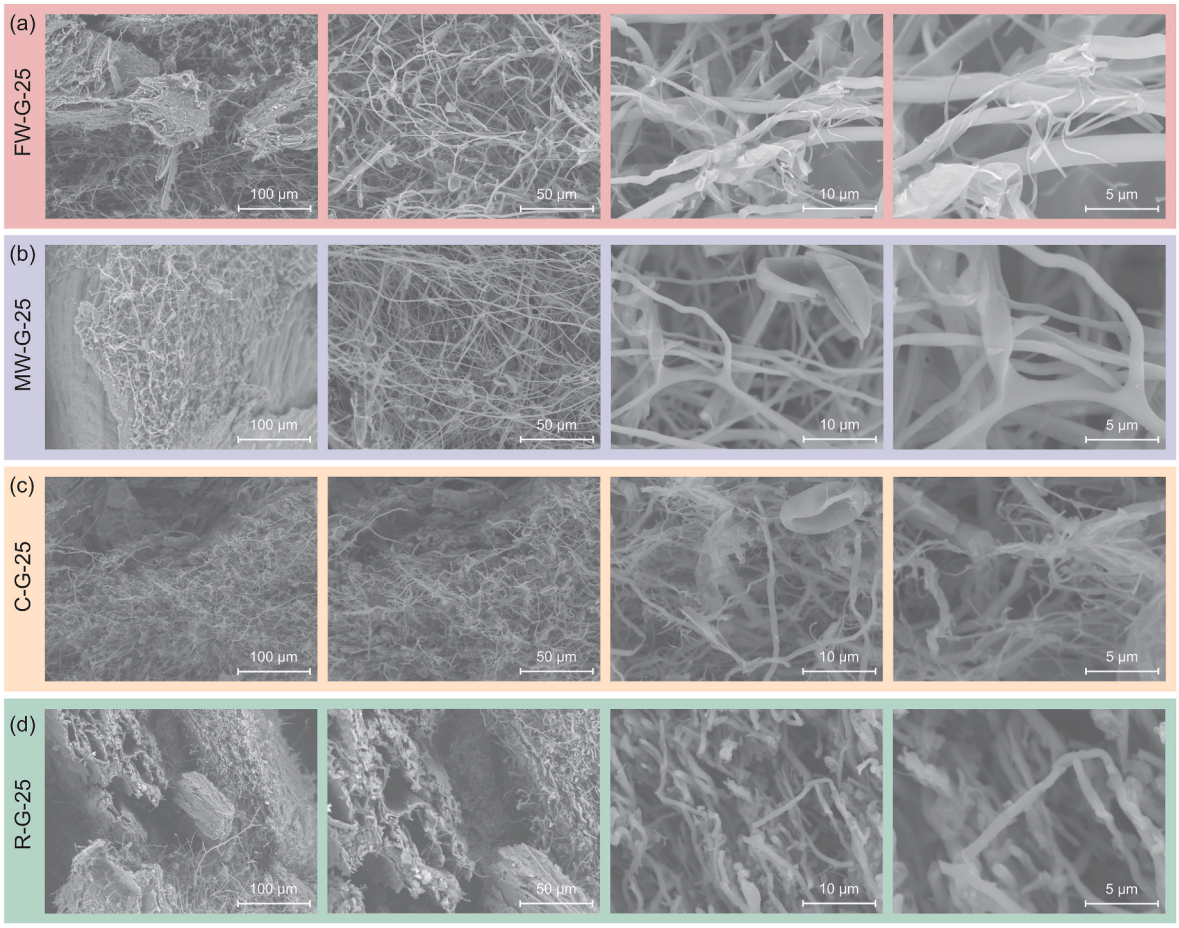

Fig. 6. SEM cross-sections of mycelium-based biocomposites grown at 25 °C on (a) fine-sized wheat bran, (b) medium-sized wheat bran, (c) spent coffee grounds, and (d) rice straw.

growth, with implications for tailoring composite performance via substrate design.

3.7. Fire performance and flammability analysis

The reaction-to-fire properties of the biocomposites were evaluated

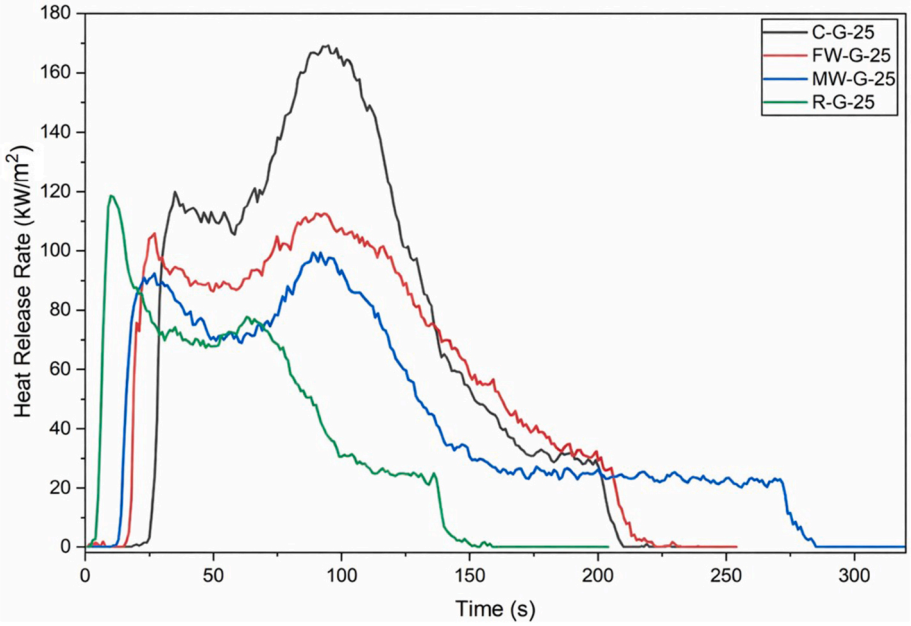

Fig. 7. Heat release rate curves of the tested biocomposites.

using cone calorimetry (ISO 5660). Key metrics analysed included peak heat release rate (PHRR), total heat release (THR), time to ignition (TTI), and total smoke production (TSP). Results are summarized in Table S5 and are shown in Fig. 7and Fig. S7. Various studies have investigated the fire performance of EPS, reporting peak heat release rates ranging from 208.0 to 446.43 kW/m^2 and total heat release values from 8.4 to 15.1 up to 42.3 MJ/m^2 [47,52–56]. Among all the samples investigated for this study, EPS still had the highest PHRR (377 kW/m^2) with moderate THR (11.2 MJ/m^2) and the longest TTI (29s). This is consistent with its well-known fire performance stemming from lack of char formation. The mycelium-based biocomposites demonstrated varied reaction-to-fire behaviors depending on substrate composition. C-G-25 showed the highest PHRR (163 kW/m^2) and THR (15.6 MJ/m^2) among the biocomposites, indicating intense combustion and limited flame retardancy, due to poor mycelial penetration and porous structure as shown in the SEM results in Fig. 6. Moreover, its high TSP (61 m^2) suggests significant smoke release during thermal decomposition. R-G-25, derived from silica-rich rice straw, ignited rapidly (TTI = 6.5 s), but exhibited the lowest THR (7.2 MJ/m^2). It also had a PHRR (119.1) statistically insignificant from those of FW-G-25 (115.3) and MW-G-25 (113.6). Despite its rapid ignition, which may be attributed to early volatile release, the inherent mineral content and low hyphal density are likely to have resulted in the reduced THR. In contrast, wheat bran-based composites (FW-G-25 and MW-G-25) showed more balanced fire performance across all the metrics. Both exhibited moderate PHRR (112–115 kW/m^2). These improvements are attributed to the denser and more continuous mycelial network, which contributed to char formation and thermal shielding, delaying combustion and suppressing flame spread. Overall, these findings emphasize the importance of substrate selection in optimizing fire performance of mycelium-based composites. While EPS remains a challenge due to its intense and toxic combustion behavior, appropriately formulated mycelium-based biocomposites, particularly those based on wheat bran, provide a more sustainable alternative for thermal insulation applications.

3.8. Cost and sustainability aspects

While this study does not primarily aim to assess the sustainability and circularity of the process, some calculations offer indicative insights into its potential environmental impact. In laboratory settings, the energy consumption for producing these biocomposites, as per the parameters specified by the manufacturer (FRIOCELL 55 - ECO line from MMM Medcenter Einrichtungen GmbH, Germany), ranges from 5.6 to 12.3 MJ/kg of biocomposites. At an industrial scale, further optimization could reduce energy consumption and associated costs. In comparison, the production of EPS is significantly more energy-intensive, requiring approximately 82 MJ/kg [52]. Moreover, the raw materials used for biocomposite production are agricultural or food industry waste products, which would otherwise require energy for disposal. Even after factoring in the embodied energy of rice straw (0.44–0.5 MJ/kg [53]) or wheat bran (3.62 MJ/kg [54]), the energy required for biocomposite production remains substantially lower than that of EPS. The cost of EPS in Europe is estimated at around €1.68/kg [55]. In contrast, the initial materials for biocomposite production are highly cost-effective or often free. For example, rice straw can be procured for €33/ton in the Philippines [53], while wheat bran can be obtained for €0.1 per kg as a promising cost-effective feedstock for biopolymer valorization [56]. Spent coffee grounds, another significant substrate, can be collected at a cost of €0.09/dry ton [57] or obtained free of charge. Assuming average global energy costs of €0.14/kWh [58], and €0.004/kg for water [59], the estimated production cost of these biocomposites ranges from €0.3 to €0.6/kg. This demonstrates that these biocomposites are economically competitive with EPS while reducing agricultural waste streams. These economic advantages of biocomposite production stand in contrast to the externalized costs of EPS manufacturing, which include high recycling and transport expenses, environmental persistence, inefficient logistics, and limited infrastructure for effective waste sorting and recovery [60]. In terms of carbon dioxide emissions, the data from the International Energy Agency (IEA) indicates a global carbon intensity of electricity generation at 0.346 kg CO_2 per kWh [61]. Consequently, the carbon footprint of biocomposites produced in this study ranges from 0.5 to 1.2 kg CO_2 eq./kg dry product. This is significantly lower than the global warming potential associated with EPS production, which is estimated at 3 kg CO_2 eq./kg product [62]. Furthermore, indirect emissions from biocomposite production are lower than EPS due to the potential for localized production, reducing transportation-related CO_2 emissions. A visual comparison of the estimated energy consumption and carbon footprint between EPS and the biocomposites developed in this study is presented in Fig. 8, highlighting approximately 89 % lower energy use and 72 % reduction in CO_2 emissions.

4. Conclusions

This study developed mycelium-based biocomposites from agro-food residues using *Ganoderma lucidum* via solid-state cultivation. Multiscale structure-property relationships were studied to link substrate composition with microstructure and performance. The main conclusions are as follows.

1. Substrate and Microstructure

Wheat bran provided the most favorable biochemical composition for mycelial growth, resulting in denser and more cohesive networks than rice straws or spent coffee grounds. All composites showed inherent surface hydrophobicity due to full surface coverage of mycelium skin, with water contact angles ranging from 106° to 120°.

2. Mechanical and Thermal Properties

Wheat bran-based biocomposites exhibited the highest mechanical performance, with compressive strength up to 449 kPa at 30 % strain and tensile modulus up to 15–25 MPa, surpassing those of EPS. TGA and hot-plate conductivity measurements confirmed that these biocomposites are suitable as porous insulation materials.

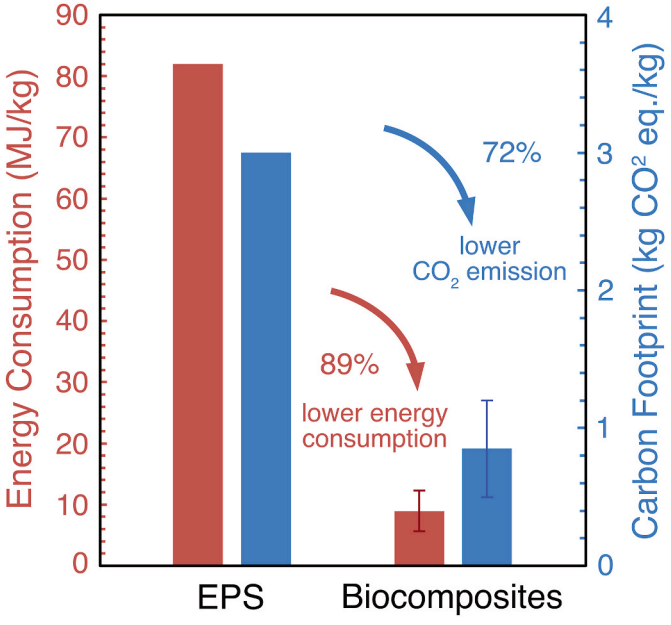

Fig. 8. Estimated energy consumption and carbon footprint of the biocomposites in this study compared with EPS.

3. Fire Performance

Cone calorimetry revealed reduced peak heat-release rates (112–115 kW/m^2) for wheat bran-based composites, surpassing EPS. The enhanced fire safety of these composites was attributed to cohesive mycelial networks and potential effective char formation.

4. Environmental Impact

These biocomposites were produced with up to 89 % lower energy input and 72 % lower carbon emissions compared to EPS.

Together, these findings establish a viable route for transforming low-value agro-food residues into scalable, fire-safer, and circular bio-based insulation materials. This work also demonstrates that a deeper understanding of fungal-substrate interactions may provide further insights into rational design of mycelium-based materials.

CRediT authorship contribution statement

Maryam Nejati: Data curation, Formal analysis, Investigation, Methodology, Visualization, Writing – original draft, Writing – review & editing. **Li Zha:** Data curation, Formal analysis, Investigation, Methodology, Validation, Visualization, Writing – original draft, Writing – review & editing. **Rhoda Afriyie Mensah:** Data curation, Formal analysis, Investigation, Writing – original draft. **Oisik Das:** Formal analysis, Investigation, Methodology, Validation, Writing – original draft, Writing – review & editing. **Antonio J. Capezza:** Conceptualization, Formal analysis, Funding acquisition, Investigation, Methodology, Supervision, Validation, Writing – original draft, Writing – review & editing. **Amparo Jiménez-Quero:** Conceptualization, Formal analysis, Funding acquisition, Investigation, Methodology, Project administration, Supervision, Validation, Writing – original draft, Writing – review & editing.

Declaration of competing interest

The authors declare that they have no known competing financial interests or personal relationships that could have appeared to influence the work reported in this paper.

Acknowledgements

The authors acknowledge funding from the Knut and Alice Wallenberg Foundation (KAW) through the Wallenberg Wood Science Center, WWSC 3.0: KAW 2021.0313; from the Swedish Research Council Formas (Project MYCOMYM 2022-00401) and the Carl Tryggers Foundation (Project CTS 22:2169). The co-finance provided to the BioRESorb team at KTH from FORMAS 2022-00362 and the feedback provided by Dr. Björn Birdsong regarding the thermal conductivity tests are acknowledged.

Appendix A. Supplementary data

Supplementary data to this article can be found online at https://doi.org/10.1016/j.mtsust.2025.101295.

Data availability

Data will be made available on request.

References

[1] A. Jimenez-Quero, E. Pollet, M. Zhao, E. Marchioni, L. Averous, V. Phalip, Fungal fermentation of lignocellulosic biomass for itaconic and fumaric acid production, J. Microbiol. Biotechnol. 27 (1) (2017) 1–8.
[2] S.R. Karade, Cement-bonded composites from lignocellulosic wastes, Constr. Build. Mater. 24 (8) (2010) 1323–1330.
[3] M. Mujtaba, L. Fernandes Fraceto, M. Fazeli, S. Mukherjee, S.M. Savassa, G. Araujo de Medeiros, et al., Lignocellulosic biomass from agricultural waste to the circular economy: a review with focus on biofuels, biocomposites and bioplastics, J. Clean. Prod. 402 (2023) 136815.
[4] K.N. Yogalakshmi, P. Sivashanmugam, S. Kavitha, R. Yukesh Kannah, J. Rajesh Banu, Lignocellulosic biomass-based pyrolysis: a comprehensive review, Chemosphere 286 (2022) 131824.
[5] C. Girometta, A.M. Picco, R.M. Baiguera, D. Dondi, S. Babbini, M. Cartabia, et al., Physico-mechanical and thermodynamic properties of mycelium-based biocomposites: a review, Sustainability 11 (1) (2019) 281.
[6] O. Robertson, Fungal Future: a Review of Mycelium Biocomposites as an Ecological Alternative Insulation Material, DS 101: Proceedings of NordDesign 2020, Lyngby, Denmark, 2020, pp. 1–13, 12th-14th August 2020.
[7] European Commission: Directorate-General for Internal Market IE, Smes, A. Oberender, T. Fruergaard Astrup, S. Frydkjær Witte, M. Camboni, EU Construction & Demolition Waste Management Protocol Including Guidelines for Pre-demolition and Pre-renovation Audits of Construction Works – Updated Edition 2024, Publications Office of the European Union, 2024 et al.
[8] A. Fråne, Lack of alternatives to fossil-based plastics in the construction sector. https://www.ivl.se/english/ivl/press/news/2021-03-19-lack-of-alternatives-to-fossil-based-plastics-in-the-construction-sector.html/, 2021. (Accessed 5 July 2025).
[9] F. Trubiano, C. Onbargi, A. Finaldi, Z. Whitlock, Fossil Fuels, the Building Industry, and Human Health, Kleinman Center for Energy Policy, Philadelphia, PA, USA, 2019.
[10] K. Yucel, C. Basyigit, C. Ozel, Thermal insulation properties of expanded polystyrene as construction and insulating materials. 15th Symposium in Thermophysical Properties, 2003, pp. 54–66.
[11] K. Rafiee, G. Kaur, S.K. Brar, Fungal biocomposites: how process engineering affects composition and properties? Bioresour. Technol. Rep. 14 (2021) 100692.
[12] M. Jones, T. Bhat, E. Kandare, A. Thomas, P. Joseph, C. Dekiwadia, et al., Thermal degradation and fire properties of fungal mycelium and mycelium - biomass composite materials, Sci. Rep. 8 (1) (2018) 17583.
[13] M. Jones, T. Bhat, T. Huynh, E. Kandare, R. Yuen, C.H. Wang, et al., Waste-derived low-cost mycelium composite construction materials with improved fire safety, Fire Mater. 42 (7) (2018) 816–825.
[14] D. Sharma, H. Le Ferrand, 3D printed gyroid scaffolds enabling strong and thermally insulating mycelium-bound composites for greener infrastructures, Nat. Commun. 16 (2025) 1–13.
[15] E. Soh, R. Fadhilla Martono, K. Wei Ng, J. Heng Teoh, A. Jain, H. Le Ferrand, et al., Comparison of the thermal performance and durability of textured mycelium-bound composite tiles made using Ganoderma lucidum and Pleurotus ostreatus, Adv. Sustain. Syst. (2025) e00528.
[16] M. Zhang, J. Xue, R. Zhang, W. Zhang, Y. Peng, M. Wang, et al., Mycelium composite with hierarchical porous structure for thermal management, Small 19 (2023) 2302827.
[17] T. Zhou, Y. Bai, H. Zhang, B. Ma, J. Yuan, X. Fan, et al., Flexible hollow-structured reinforced mycelium insulation material and its performance, Adv. Mater. Technol. 10 (2025) 2500315.
[18] Z. Merali, S.R.A. Collins, A. Elliston, D.R. Wilson, A. Käsper, K.W. Waldron, Characterization of cell wall components of wheat bran following hydrothermal pretreatment and fractionation, Biotechnol. Biofuels 8 (1) (2015) 23.
[19] S.N. Harun, M.M. Hanafiah, N.M. Noor, Rice straw utilisation for bioenergy production: a brief overview, Energies (2022).
[20] F. Taleb, M. Ammar, Mb Mosbah, Rb Salem, Y. Moussaoui, Chemical modification of lignin derived from spent coffee grounds for methylene blue adsorption, Sci. Rep. 10 (1) (2020) 11048.
[21] S. Manan, M.W. Ullah, M. Ul-Islam, O.M. Atta, G. Yang, Synthesis and applications of fungal mycelium-based advanced functional materials, J. Bioresour. Bioprod. 6 (1) (2021) 1–10.
[22] E. Camilleri, S. Narayan, D. Lingam, R. Blundell, Mycelium-based composites: an updated comprehensive overview, Biotechnol. Adv. (2025) 108517.
[23] A. Martínez-Abad, A. Jiménez-Quero, J. Wohlert, F. Vilaplana, Influence of the molecular motifs of mannan and xylan populations on their recalcitrance and organization in spruce softwoods, Green Chem. 22 (12) (2020) 3956–3970.
[24] Plastics ACD-o. Standard Test Method for Compressive Properties of Rigid Cellular Plastics, ASTM International, 2004.
[25] International A. ASTM D638-14, Standard Test Method for Tensile Properties of Plastics, ASTM International, 2015.
[26] T.O. Blomfeldt, F. Nilsson, T. Holgate, J. Xu, E. Johansson, M.S. Hedenqvist, Thermal conductivity and combustion properties of wheat gluten foams, ACS Appl. Mater. Interfaces 4 (3) (2012) 1629–1635.
[27] R. Bird, Transport phenomena wiley. Transport Phenomena, second ed., Wiley, 2006.
[28] ISO 5660-1:2015, Reaction-To-Fire Tests — Heat Release, Smoke Production and Mass Loss Rate — Part 1: Heat Release Rate (Cone Calorimeter Method) and Smoke Production Rate (Dynamic Measurement), third ed., International Organization for Standardization, Geneva, 2015.
[29] P. Kapoor, B. Sharma, Studies on different growth parameters of Ganoderma lucidum, Int J Sci Environ Tech 3 (2014) 1515–1524.
[30] C. Jayasinghe, A. Imtiaj, H. Hur, G.W. Lee, T.S. Lee, U.Y. Lee, Favorable culture conditions for mycelial growth of Korean wild strains in Ganoderma lucidum, Mycobiology 36 (1) (2008) 28–33.
[31] D.S. Mardijanti, E.N. Megantara, A. Bahtiar, S. Sunardi, Turning the Cocopith waste into myceliated biocomposite to make an insulator, Int. J. Biomater. 2021 (2021) 6630657.

[32] R. Bakker, H. Elbersen, R. Poppens, J.P. Lesschen, Rice straw and wheat straw-potential feedstocks for the biobased economy. (2013).
[33] Z. Zheng, K. Shetty, Solid-state production of beneficial fungi on apple processing wastes using glucosamine as the indicator of growth, J. Agric. Food Chem. 46 (2) (1998) 783–787.
[34] Z. Li, C. Zhang, Y. Zhang, W. Zeng, I. Cesarino, Coffee cell walls—composition, influence on cup quality and opportunities for coffee improvements, Food Qual. Saf. 5 (2021).
[35] A.N. Brylev, D.K. Adylov, G.G. Tukhtaeva, N.A. Kamal'dinova, L.D. Abidova, D. A. Rakhimov, Polysaccharides of rice straw, Chem. Nat. Compd. 37 (6) (2001) 569–570.
[36] A. Nandiyanto, T. Rahman, M. Fadhlulloh, A. Abdullah, I. Hamidah, B. Mulyanti, Synthesis of silica particles from rice straw waste using a simple extraction method. IOP Conference Series: Materials Science and Engineering, IOP Publishing, 2016 012040.
[37] L. Peng, J. Yi, X. Yang, J. Xie, C. Chen, Development and characterization of mycelium bio-composites by utilization of different agricultural residual byproducts, J. Bioresour. Bioprod. 8 (1) (2023) 78–89.
[38] M.L.M. Budlayan, J.N. Patricio, J.P. Lagare-Oracion, S.D. Arco, A.C. Alguno, A. Basilio, et al., Improvised centrifugal spinning for the production of polystyrene microfibers from waste expanded polystyrene foam and its potential application for oil adsorption, J. Eng. Appl. Sci. 68 (2021) 1–11.
[39] P.S. Brown, B. Bhushan, Mechanically durable liquid-impregnated honeycomb surfaces, Sci. Rep. 7 (2017) 1–6.
[40] F.V.W. Appels, J. Dijksterhuis, C.E. Lukasiewicz, K.M.B. Jansen, H.A.B. Wösten, P. Krijgsheld, Hydrophobin gene deletion and environmental growth conditions impact mechanical properties of mycelium by affecting the density of the material, Sci. Rep. 8 (1) (2018) 4703.
[41] R.M. Escaleira, M.J. Campos, M. Alves, Mycelium-based composites: a new approach to sustainable materials. Sustainability and Automation in Smart Constructions: Proceedings of the International Conference on Automation Innovation in Construction (CIAC-2019), Springer, Leiria, Portugal, 2021, pp. 261–266.
[42] Z. Tacer-Caba, J.J. Varis, P. Lankinen, K.S. Mikkonen, Comparison of novel fungal mycelia strains and sustainable growth substrates to produce humidity-resistant biocomposites, Mater. Des. 192 (2020) 108728.
[43] P.S. Liu, G.F. Chen, Chapter one - general introduction to porous materials, in: P. S. Liu, G.F. Chen (Eds.), Porous Materials, Butterworth-Heinemann, Boston, 2014, pp. 1–20.
[44] M.E. Hajam, W. Sun, I. Hafez, C. Howell, M. Tajvidi, In situ growth of mycelium in a lignocellulosic scaffold enabled by cellulose nanofibrils for lightweight insulation, Compos. Appl. Sci. Manuf. 199 (2025) 109223.
[45] E. Elsacker, S. Vandelook, J. Brancart, E. Peeters, L. De Laet, Mechanical, physical and chemical characterisation of mycelium-based composites with different types of lignocellulosic substrates, PLoS One 14 (7) (2019) e0213954.
[46] A.K. Sakhiya, A. Anand, V.K. Vijay, P. Kaushal, Thermal decomposition of rice straw from rice basin of India to improve energy-pollution nexus: kinetic modeling and thermodynamic analysis, Energy Nexus 4 (2021) 100026.
[47] S.P. Bhoite, J. Kim, W. Jo, P.H. Bhoite, S.S. Mali, K.H. Park, et al., Expanded polystyrene beads coated with intumescent flame retardant material to achieve fire safety standards, Polymers 13 (2021) 2662.
[48] J.A. López Nava, J. Méndez González, X. Ruelas Chacón, J.A. Nájera Luna, Assessment of edible fungi and films bio-based material simulating expanded polystyrene, Mater. Manuf. Process. 31 (8) (2016) 1085–1090.
[49] J. Wildman, A. Shea, P. Walker, D. Henk, Extrinsic and intrinsic determinants of thermal conductivity in mycelium composites, Build. Serv. Eng. Res. Tecnol. 46 (2025) 317–338.
[50] N.H. Ramli Sulong, S.A.S. Mustapa, M.K. Abdul Rashid, Application of expanded polystyrene (EPS) in buildings and constructions: a review, J. Appl. Polym. Sci. 136 (2019) 47529.
[51] G. De, L. Yang, J. Lee, Y.H. Wu, Z. Tian, Z. Qin, Mycelium–coir-based composites for sustainable building insulation, J. Mater. Chem. A 13 (2025) 9694–9707.
[52] C. Hill, A. Norton, J. Dibdiakova, A comparison of the environmental impacts of different categories of insulation materials, Energy Build. 162 (2018) 12–20.
[53] V.H. Nguyen, S. Topno, C. Balingbing, V.C.N. Nguyen, M. Röder, J. Quilty, et al., Generating a positive energy balance from using rice straw for anaerobic digestion, Energy Rep. 2 (2016) 117–122.
[54] M. Maysami, W. Berg, Comparison of energy intensity of different food materials and their energy content, Food Res. 5 (1) (2021) 168–174.
[55] BusinessAnalytiq, Expandable polystyrene (EPS) price index, in: https://businessanalytiq.com/procurementanalytics/index/expandable-polystyrene-eps-price-index/, 2023. (Accessed 5 July 2025).
[56] D. Rossi, S. Rossi, P. Cinelli, M. Seggiani, Emerging opportunities in the valorisation of wheat bran byproduct as additive in polymer composite materials, Mater. Today Sustain. (2024) 100832.
[57] A. Mukherjee, J.A. Okolie, C. Niu, A.K. Dalai, Techno – economic analysis of activated carbon production from spent coffee grounds: comparative evaluation of different production routes, Energy Convers. Manag. X 14 (2022) 100218.
[58] GlobalPetrolPrices. Electricity prices. https://www.globalpetrolprices.com/electricity_prices/, 2023. (Accessed 5 July 2025).
[59] HolidуGmbH, The water price index (EUR). https://www.holidu.com/magazine/water-price-index-intl/, 2021. (Accessed 5 July 2025).
[60] Z. Xu, D. Sun, J. Xu, R. Yang, J.D. Russell, G. Liu, Progress and challenges in polystyrene recycling and upcycling, ChemSusChem 17 (17) (2024) e202400474.
[61] IEA, Carbon intensity of electricity generation in selected regions in the sustainable development scenario, 2000-2040. https://www.iea.org/data-and-statistics/charts/carbon-intensity-of-electricity-generation-in-selected-regions-in-the-sustainable-development-scenario-2000-2040, 2020. (Accessed 5 July 2025).
[62] Y. Lim, T. Izhar, I. Zakarya, S. Yusuf, S. Zaaba, M. Mohamad, Life cycle assessment of expanded polystyrene. IOP Conference Series: Earth and Environmental Science, IOP Publishing, 2021 012030.
[63] M.D. Hossain, M.K. Hassan, M. Akl, S. Pathirana, P. Rahnamayiezekavat, G. Douglas, et al., Fire behaviour of insulation panels commonly used in high-rise buildings, Fire 5 (3) (2022) 81.
[64] W. An, L. Jiang, J. Sun, K.M. Liew, Correlation analysis of sample thickness, heat flux, and cone calorimetry test data of polystyrene foam, J. Therm. Anal. Calorimetry 119 (2015) 229–238.
[65] M.E. Li, Y.W. Yan, H.B. Zhao, R.K. Jian, Y.Z. Wang, A facile and efficient flame-retardant and smoke-suppressant resin coating for expanded polystyrene foams, Compos. B Eng. 185 (2020) 107797.
[66] X. Shao, Y. Du, X. Zheng, J. Wang, Y. Wang, S. Zhao, et al., Reduced fire hazards of expandable polystyrene building materials via intumescent flame-retardant coatings, J. Mater. Sci. 55 (2020) 7555–7572.
[67] Q. Xu, C. Jin, G. Griffin, Y. Jiang, Fire safety evaluation of expanded polystyrene foam by multi-scale methods, J. Therm. Anal. Calorimetry 115 (2014) 1651–1660.